JOURNAL OF MATERIALS SCIENCE 27 (1992) 6379–6386

Strengthening of cement foams

T. D. TONYAN, L. J. GIBSON
Department of Civil Engineering, Massachusetts Institute of Technology, Cambridge, MA 02139, USA

Lightweight cellular concretes are attractive building materials for a number of reasons: they offer a unique combination of moderate thermal insulation and stiffness, low cost and incombustibility. They have relatively low strength, however, and are brittle. In this paper we describe the behaviour of composite cement/polystyrene foams with improved strength and ductility.

1. Introduction

Low-density cement foams (160–240 kg m^{-3}) have a number of properties which make them attractive for the cores of structural sandwich panels. Compared to polymer foam cores, they are stiff, cheap and incombustible. Their thermal conductivity is higher than that of polymer foam cores, but because of their low cost, this can be compensated for by the use of thicker sections. Their main limitation is their brittleness and low tensile strength. This paper describes a study to improve the strength and ductility of cement foams through the development of a composite cement/polystyrene foam.

The mechanical properties of foams are largely controlled by bending of the cell walls [1]. The stiffness of a foam is controlled by the flexural rigidity of the cell wall, EI, while the strength is controlled by its modulus of rupture, σ_{fs}, and section modulus, S. In plain cement foams, such as those described in the previous, companion paper [2], the cell walls are roughly rectangular in cross-section, an inefficient shape for resisting bending loads. The bending resistance could be improved if the cross-section could be made into an "I" or a sandwich section. While it is not practical to make cell walls into I beams, it is possible to produce a sandwich-like structure on a cell wall level. Consider the introduction of a high volume-fraction of large diameter, thin-walled, stiff hollow spheres into a cement foam, as illustrated in Fig. 1a. The thin walls of the large diameter spheres act as the faces of the sandwich while the smaller diameter cells of the cement foam act as a foam core. We expect such a microstructure to be efficient in resisting bending loads.

We have been able to make cement foams with such a sandwich cell wall by introducing 50% by volume of 3–5 mm diameter, 48 kg m^{-3} expanded polystyrene (EPS) beads into a matrix of 320 kg m^{-3} cement foam with a median cell size of roughly 260 μm. The expanded polystyrene bead acts as a form for a 20–50 μm thick coating of fully dense cement paste. This thin layer of neat cement paste acts as the faces of the sandwich while the foamed cement acts as the core (Fig. 1b). The expanded polystyrene bead, with its low mechanical properties, does not contribute to the mechanical properties of the composite. The properties of the cement composite foam arise entirely from the sandwich structure of the cell wall and the properties of the cement.

2. Experimental procedure

The processing of plain cement foams was described previously [2]. The cement matrix in the composite cement/polystyrene foam was designed to have a nominal density of 320 kg m^{-3}. The expanded polystyrene beads were added to the cement slurry prior to mixing in the preformed foam. A fully dense cement paste

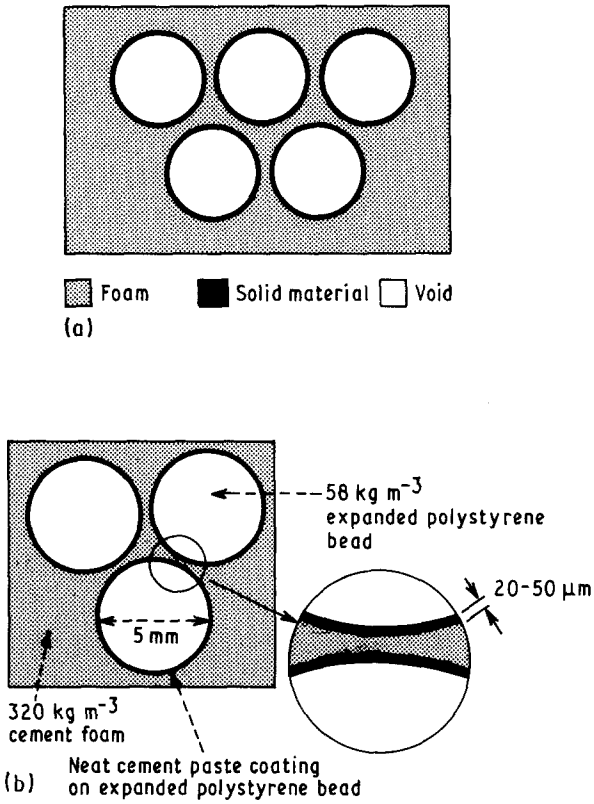

Figure 1 (a) Composite foam with thin-walled hollow spheres in a matrix of a smaller-celled foam. (b) Composite cement/expanded polystyrene bead foam.

0022–2461

coating remained around the beads, while the interstices were filled with the cement foam, producing the structure shown in Fig. 1b. The volume fractions of polystyrene beads added to the 320 kg m^{-3} cement foam were nominally 0%, 20%, 30%, 45%, 50% and 52%. Various types of beads were used in trial batches, including 6.4 mm diameter, 192 kg m^{-3} expanded polystyrene spheres coated with fibre-reinforced epoxy, 60 μm diameter, 120 kg m^{-3} hollow glass microspheres, and 6–12 mm diameter, 576 kg m^{-3} ceramic spheres. The expanded polystyrene beads gave the most suitable microstructure and were light and inexpensive. Cylinders (152 mm diameter, 305 mm high) and beams (51 mm × 51 mm × 203 mm) were cast in the manner described previously [2].

The microstructure of the cement/polystyrene foam composites were characterized using the techniques described previously [2] for plain cement foams. The beads ranged in density from 48–67 kg m^{-3}, with a mean of 58 kg m^{-3}; they ranged in diameter from 3.4–5.6 mm, with a mean of 4.4 mm. The composites were tested in compression and in bending to measure the Young's modulus, the compressive strength and the modulus of rupture, as described previously [2]. A minimum of three beam and cylinder specimens were tested at nominal volume fractions of beads of 20%, 30%, 40% and 50%.

The mechanical properties of the polystyrene beads were estimated using the models of Gibson and Ashby [1]. Young's modulus is estimated from

$$\frac{E^*}{E_s} = \left[\frac{\rho^*}{\rho_s}\right]^2 \quad (1)$$

and the compressive strength is estimated from

$$\frac{\sigma^*_{el}}{E_s} = 0.05\left[\frac{\rho^*}{\rho_s}\right]^2 \quad (2)$$

for failure by elastic buckling, and from

$$\frac{\sigma^*_{pl}}{\sigma_{ys}} = 0.3\left[\frac{\rho^*}{\rho_s}\right]^{3/2} \quad (3)$$

for failure by plastic yielding, where E^*, ρ^* and σ^*_{pl} are the Young's modulus, density and plastic compressive strength of the expanded polystyrene and E_s, ρ_s and σ_{ys} are those of the solid polystyrene. σ^*_{el} is the elastic buckling strength of the foam. For polystyrene, E_s ranges from 1.4–3.0 GPa, $\rho_s = 1050$ kg m^{-3} and σ_{ys} ranges from 30–80 MPa. For the polystyrene beads used to make the composite foam, $\rho^* = 58$ kg m^{-3}. The Young's modulus of the beads is estimated to be in the range 4.1–9.0 MPa, the elastic compressive strength in the range 0.21–0.46 MPa, and the plastic compressive strength in the range of 0.12–0.31 MPa. Uniaxial loading of a half sphere revealed permanent deformation at small strains, consistent with the above estimation of a lower plastic than an elastic compressive strength. For comparison, the Young's modulus and compressive strength of the plain 320 kg m^{-3} cement foam are about 140 and 0.34 MPa, respectively.

3. Results

Micrographs of a 320 kg m^{-3} cement foam with 30% and 50% by volume of 58 kg m^{-3} expanded polystyrene beads are shown in Fig. 2a and b. The densities of the composites were 241 and 192 kg m^{-3}, respectively. The polystyrene sphere was coated with a thin layer of neat cement paste; this layer was measured to be 10–100 μm thick, with a mean of 20–50 μm (Fig. 2c, d). Confirmation of the presence of this continuous coating of cement around the surface of the sphere was obtained by painting the surface of the composite with acetone which dissolved the polystyrene spheres. Visual inspection revealed that a continuous coating of cement was present in almost every case. Large coalesced voids in the cement foam matrix still account for roughly 50% of the porosity; however, they appear only in the larger interstitial spaces between the polystyrene spheres. The sandwich cell wall of the composite foam had a span of 1–3 mm, a core thickness ranging from 100–500 μm, and a face thickness that varied from 20–50 μm. The density of the cement foam core of the sandwich was held as close to 320 kg m^{-3} as possible; it ranged from 290–350 kg m^{-3}.

Typical compressive load–displacement curves are shown in Fig. 3a and b. As the volume fraction of spheres was increased from 20% to 50%, the initial slope of the curve remained approximately constant, the failure load increased from 1100 N to 1500 N and the post-failure load increased slightly. Typical bending load–displacement curves are shown in Fig. 3c and d. As the volume fraction of spheres increased from 10% to 50%, both the ultimate load and the strain at the ultimate load increased dramatically: the load from 80 N to 200 N, and the deflection from 0.25 mm to 1.1 mm.

The Young's modulus and the specific Young's modulus of the cement/polystyrene composite foams are plotted as a function of the volume fraction of spheres in Fig. 4. Data for the plain cement foams of equal density are included for comparison. The Young's modulus of the composite foams initially fall, and then increase with increasing volume fractions of spheres, while the moduli of the plain cement foams steadily decrease. The Young's modulus per unit density increases to roughly 150% of the value for the plain cement foam as the volume fraction of spheres is increased to 50%.

The compressive strength of the composite foam displays the same trends (Fig. 5): compressive strength at first decreases, and then increases, with increasing volume fractions of spheres. At the highest volume fractions of spheres (52%) the compressive strength of the composite is slightly higher than that of the plain cement foam, while the density is reduced by 60%. The specific compressive strength of the composite with 50% spheres is roughly double that of the plain cement foam.

Both the modulus of rupture and the specific modulus of rupture of the composite foam steadily increase with increasing volume fraction of spheres (Fig. 6). At the highest volume fraction, the specific modulus of rupture is almost five times that of the

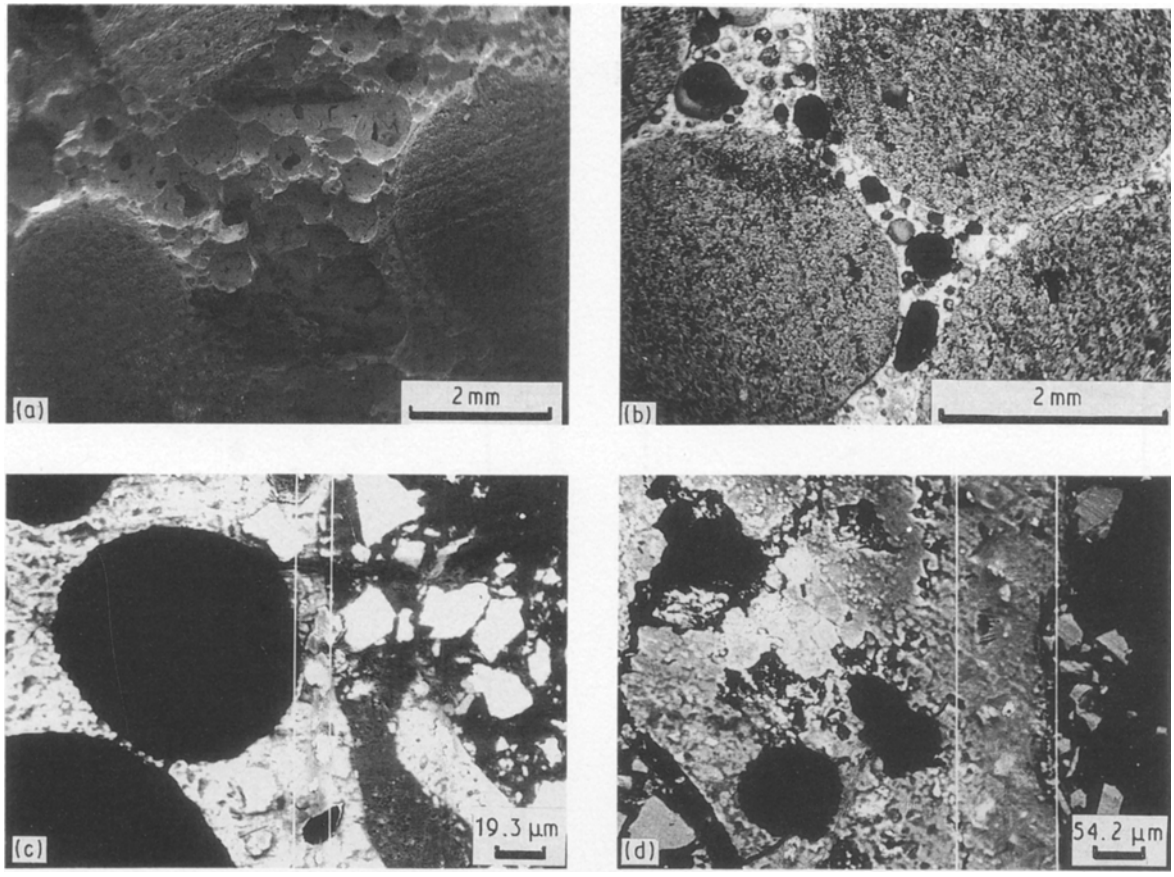

Figure 2 Micrographs of composite cement/expanded polystyrene bead foams with (a) 30% and (b) 50% by volume of EPS. (c, d) Neat cement paste layer surrounding the expanded polystyrene bead.

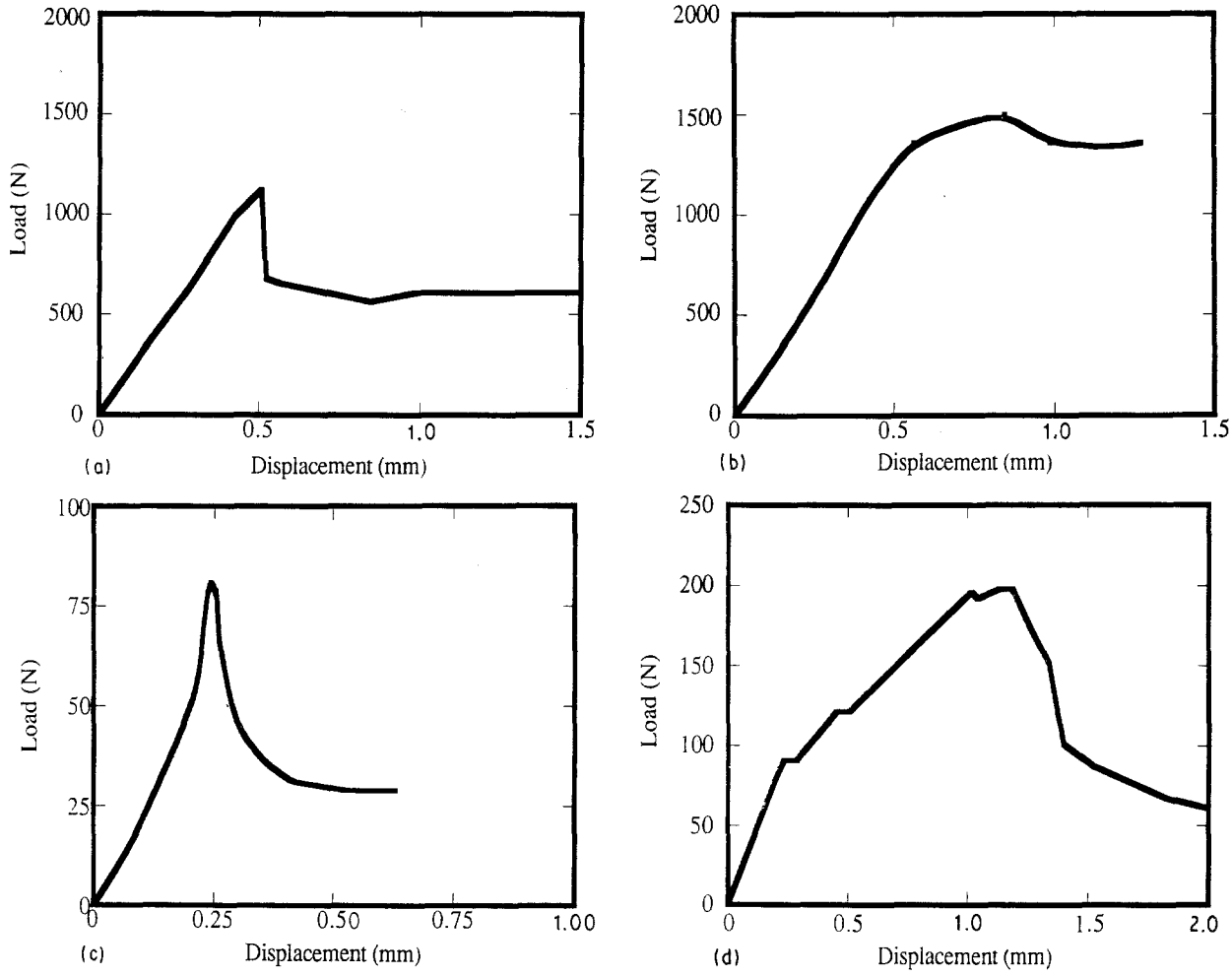

Figure 3 Load–displacement curves for cement foams with (a) 20% EPS beads, uniaxial compression, (b) 50% EPS beads, uniaxial compression, (c) 10% EPS beads, three-point bending and (d) 50% EPS beads, three-point bending.

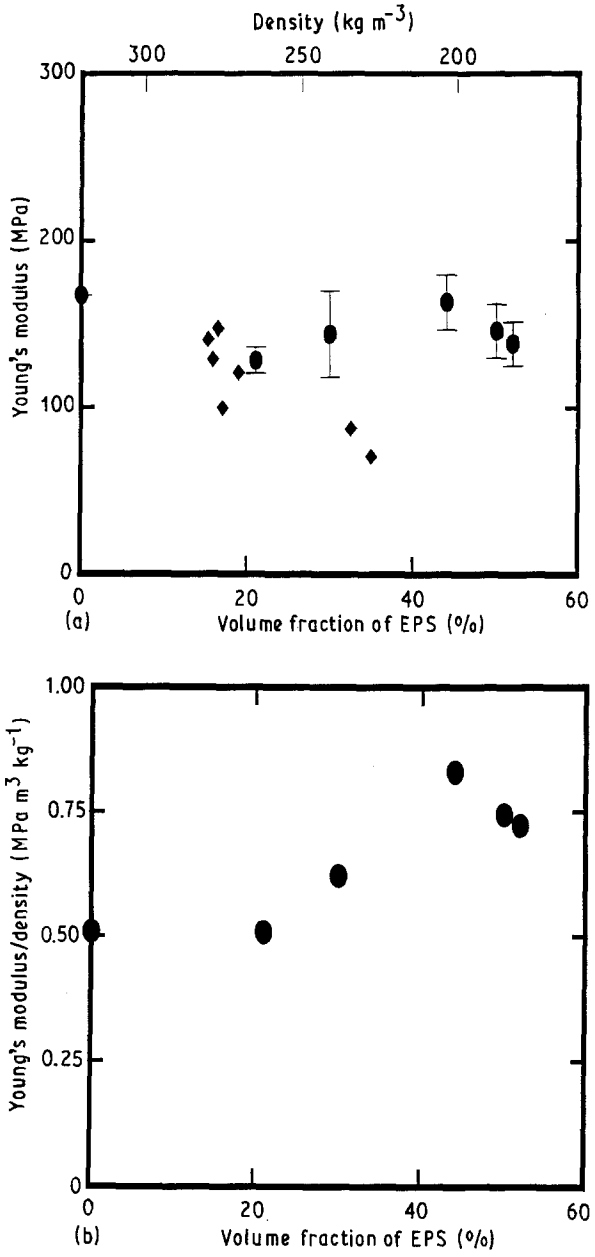

Figure 4 (a) Young's modulus and (b) specific Young's modulus plotted against volume fraction of expanded polystyrene beads. (a) (●) Average results, (◆) data for plain cement foams of the same density.

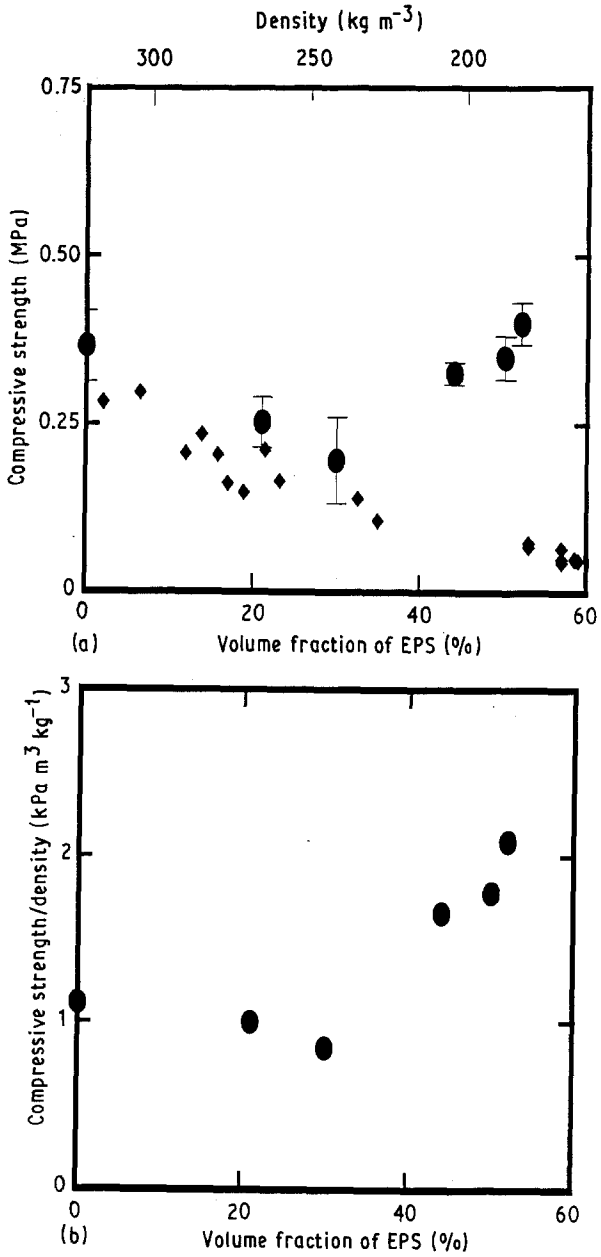

Figure 5 (a) Compressive strength and (b) specific compressive strength plotted against volume fraction of expanded polystyrene beads. (a) (●) Average results, (◆) data for plain cement foams of the same density.

plain cement foam. The modulus of rupture of the 50% volume fraction of spheres composite is roughly equal to the compressive strength, suggesting that there are no cracks larger than the cell size in the cement foam matrix. Visual inspection revealed that failure occurred in the cement foam matrix.

4. Discussion

The introduction of high volume fractions of spheres into the cement foam produces sandwich-like cell walls: the layers of neat cement paste surrounding the spheres act as the faces of the sandwich, while the 320 kg m^{-3} foamed cement acts as the core. Both the relative dimensions and the relative material properties are typical of a sandwich plate: the ratios of the face thickness and the core thickness to the span are roughly $f/l = 0.015$–0.025 and $c/l = 0.1$–0.4, respectively; the ratio of the face thickness to the core thickness, f/c, is roughly 0.1–0.2; the relative density of the foamed cement core is 0.19; and the ratio of the core shear modulus to the face Young's modulus is about 0.011.

The compressive load–deflection curves for cement foam composites with 20% and 52% volume fraction of spheres are shown in Fig. 3a and b. Initial behaviour is linear elastic. After the peak stress the load falls to a roughly constant stress plateau. As the volume fraction of spheres increases the drop in load after the peak stress becomes less sudden and the plateau stress is a higher proportion of the peak stress: at 0% spheres, the plateau stress is 50% of the peak stress (Fig. 2 in [2]), at 20% spheres, the plateau stress is 60% of the peak stress (Fig. 3a) and at 52% spheres, the plateau stress is 90% of the peak stress (Fig. 3b). The polystyrene beads may act as an elastic founda-

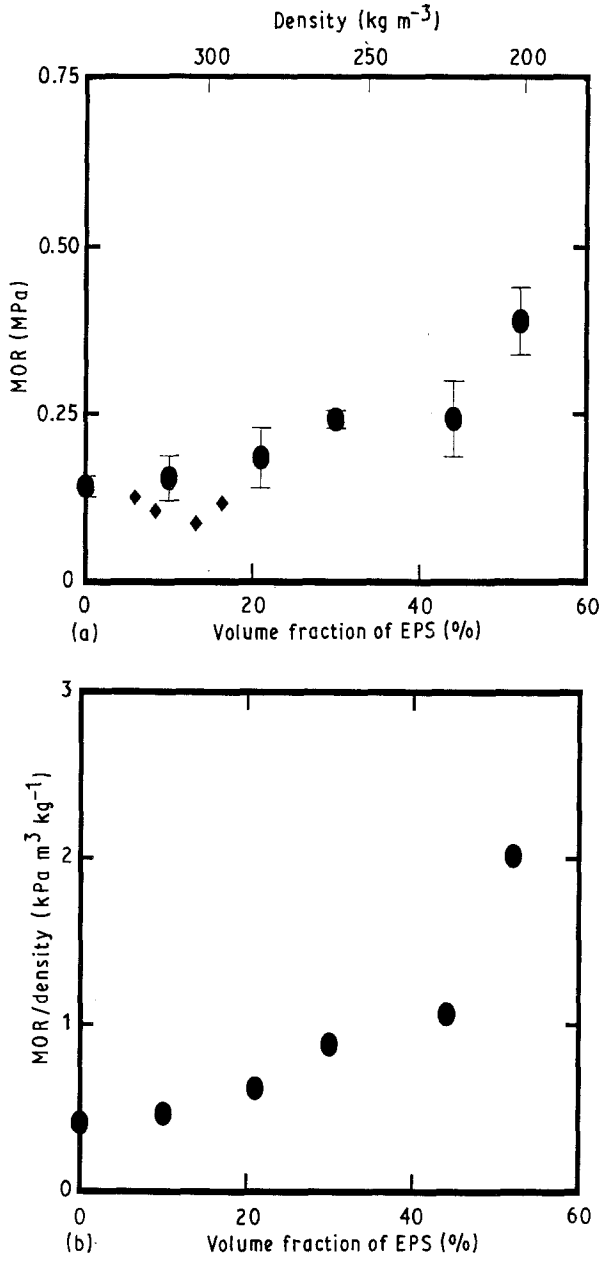

Figure 6 (a) Modulus of rupture and (b) specific modulus of rupture plotted against volume fraction of expanded polystyrene beads. (a) (●) Average results, (◆) data for plain cement foams of the same density.

tion for the bending of the cement sandwich elements; as a result they may distribute the load over the sandwich member, increasing its post-peak load-carrying capacity. The increase in post-peak strength is an attractive feature of the composite cement foam with foamed polystyrene spheres.

The Young's modulus of the cement foam composites is plotted against the volume fraction of polystyrene spheres in Fig. 4a. The modulus of the plain 320 kg m^{-3} cement foam is 170 MPa. It falls to 130 MPa as the volume fraction of spheres is increased to 21%. At 30% spheres, it increases to 140 MPa, and at 40% spheres, it rises further to 160 MPa. At 50% spheres, it remains higher than 140 MPa.

At low volume fractions of spheres, the separation between the spheres is relatively large, and no sandwich effect is produced. The spheres simply act as voids as their modulus is much less than that of the 320 kg m^{-3} cement foam; the result is that the composite modulus decreases at low volume fractions of spheres. As the volume fraction of spheres increases, the cell walls become more sandwich-like, increasing their bending stiffness and the overall modulus of the composite. At a volume fraction of spheres of 45% the modulus of the composite is almost equal to that of the plain 320 kg m^{-3} cement foam, even though the density of the composite is only 216 kg m^{-3}. The volume fraction of spheres is limited by the packing density at which the spheres touch (for randomly packed spheres of the same size this limiting volume fraction is 62%). At very high volume fractions of spheres, the thickness of the sandwich wall at its midpoint approaches zero, eliminating its effectiveness. Qualitatively, then, we might expect the modulus of a cement foam/polystyrene sphere composite to vary with the volume fraction of spheres as follows. At low volume fractions, the spheres simply act as voids, reducing the modulus. As the volume fraction is increased to some intermediate range, the cell walls become sandwich-like, increasing their bending stiffness and the Young's modulus of the composite, and at very high volume fractions of spheres, the wall thickness at its midpoint vanishes, reducing the modulus. Our data for the Young's modulus suggests that the sandwich effect occurs at volume fractions of spheres between 30% and 50%, with the most efficient microstructure being the composite with approximately 45% spheres. The specific modulus of the composites is plotted against the volume fraction of spheres in Fig. 4b; the composite with 45% spheres has a specific Young's modulus 63% higher than the plain 320 kg m^{-3} cement foam.

The behaviour of a foam with sandwich cell walls can be modelled by modifying existing models for foams with homogeneous cell walls. Consider Gibson and Ashby's [1] model for the elastic moduli of a closed cell foam in which the cell faces deform by bending (as is the case for a brittle cement foam in which the plate deflection is small compared with its span) (Fig. 7a, b). The faces of the cell are modelled as plates of thickness, t, and span, l, made of a solid material of Young's modulus, E_s (Fig. 7c). Under a load, P, the plate deflects by

$$\delta = \frac{12Pl^3}{B_1 E_s l t^3} \tag{4}$$

where B_1 is a constant depending on the loading geometry. Because the stress, $\sigma \propto P/l^2$ and the strain, $\varepsilon \propto \delta/l$, the Young's modulus, E_h^*, of the closed-cell foam with homogeneous cell walls is then

$$E_h^* \propto \frac{B_1 E_s}{12}\left(\frac{t}{l}\right)^3 \tag{5}$$

The modulus of a closed-cell foam with sandwich cell walls can be calculated in a similar fashion, replacing Equation 4 with the equation for the deflection of a sandwich plate

$$\delta = \frac{2Pl^3}{B_1 E_f f l c^2} + \frac{Pl}{B_2 G_c l c} \tag{6}$$

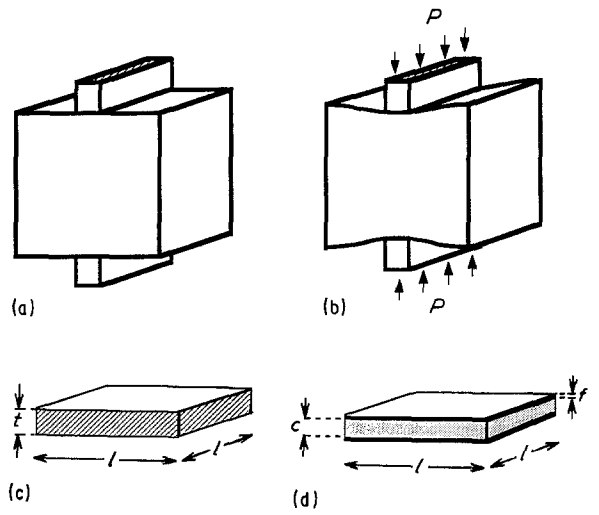

Figure 7 (a) A cubic cell of a closed-cell foam, (b) plate bending of the face of the closed-cell foam under uniaxial compression, (c) homogeneous cell wall of thickness, t, and (d) sandwich cell wall of face thickness, f, and core thickness, c.

where f is the sandwich face thickness, c is the sandwich core thickness, E_f is the Young's modulus of the face, G_c is the shear modulus of the core, and B_1 and B_2 are constants relating to the loading geometry (Fig. 7d). The Young's modulus of the closed-cell foam with sandwich cell walls is then

$$E^*_{sb} \propto \left[\frac{2}{B_1 E_f (f/l)(c/l)^2} + \frac{1}{B_2 (c/l) G_c}\right]^{-1} \quad (7)$$

Assuming that the foams with homogeneous and with sandwich walls have similar cell geometries, the constants of proportionality in Equations 5 and 7 are equal. The ratio of the Young's moduli for the foams with sandwich beam and homogeneous cell walls is then:

$$\frac{E^*_{sb}}{E^*_h} = 12(l/t)^3 \Big/ \left\{B_1 E_s \left[\frac{2}{B_1 E_f (f/l)(c/l)^2} + \frac{1}{B_2 G_c (c/l)}\right]\right\} \quad (8)$$

The homogeneous and sandwich cell wall foams have the same mass if

$$\rho_s \frac{t}{l} = 2\rho_f \frac{f}{l} + \frac{c}{l}\rho_c \quad (9)$$

where ρ_s is the density of the solid, homogeneous cell wall (Fig. 7c) and ρ_f and ρ_c are those of the face and core of the sandwich cell wall (Fig. 7d).

Here, we compare the moduli of the cement foams with sandwich cell walls, described in this paper, with those of cement foams with homogeneous cell walls, described in our previous paper [2]. For the materials tested, $E_s = E_f = 5.80$ GPa, $\rho_s = \rho_f = 1520\,\mathrm{kg\,m^{-3}}$, $f/l = 0.008$–0.020, $c/l = 0.4$–0.6, $\rho_c = 320\,\mathrm{kg\,m^{-3}}$ and $G_c/E_f = 0.012$. We estimate that, roughly speaking, each cell wall acts as a beam fixed at both ends, loaded at the ends such that one end translates relative to the other: for this configuration, $B_1 = 12$ and $B_2 = 1$.

Ratios of the Young's moduli of the cement foam with sandwich beam cell walls to that of the cement foam with homogeneous cell walls, calculated using Equations 8 and 9, are shown in Fig. 8, for values of f/l in the measured range. Superimposed on the two curves are solid lines indicating the measured values of the modular ratio, for volume fractions of spheres of 0.3, 0.4 and 0.5. Although it is difficult to measure accurately values of the core thickness to span ratio, c/l, the calculations suggest that for $V_s = 0.3$, $0.44 < c/l < 0.6$; for $V_s = 0.4$, $0.27 < c/l < 0.45$; and for $V_s = 0.5$, $0.43 < c/l < 0.24$. Estimates of c/l based on both a sphere in a cube and a sphere in a pentagonal dodecahedron indicate that for $V_s = 0.3$, $0.6 < c/l < 0.64$; for $V_s = 0.4$, $0.4 < c/l < 0.52$; and for $V_s = 0.5$, $0.3 < c/l < 0.4$. All three ranges are consistent with the values of c/l suggested by the calculations (Fig. 8). The model appears to explain well the results for the Young's modulus. The introduction of a sandwich cell wall structure increases the Young's modulus of the cement foam over that for a foam with a homogeneous cell wall structure for foams of the same weight.

The compressive strength of the composite cement/polystyrene sphere foams is plotted against the volume fraction of spheres in Fig. 5a. The strength decreases as the volume fraction of spheres is increased up to 30% and then increases at higher volume fractions. At 52% spheres, the compressive strength of the composite is slightly higher than the plain $320\,\mathrm{kg\,m^{-3}}$ cement foam, even though the density has been reduced to $208\,\mathrm{kg\,m^{-3}}$ by the introduction of the spheres. The trend is similar to that observed for the Young's modulus. At low volume fractions of polystyrene beads the separation between the beads is large and no sandwich effect is produced; the low-strength beads simply act as voids to reduce the strength of the composite (note that the composite strength is only slightly higher than that of the plain cement foam of the same density). But at higher volume fractions, the cell walls become sandwich-like, increasing their bending resistance and strength. The specific compressive strength is plotted against volume fraction of spheres in Fig. 5b; the composite with 52% spheres is the most efficient.

The ratio of the strength of a foam with sandwich cell walls to that of one with homogeneous cell walls can be calculated in the same manner as the modular ratio. The compressive strength of the foam with homogeneous cell walls, σ^*_h is reached when the maximum tensile stress in the bent cell walls equals the modulus of rupture of the cell wall, σ_{fs}. Taking the maximum tensile stress proportional to the maximum moment divided by the section modulus, we find, referring to Fig. 7c

$$\sigma^*_h = \frac{\sigma_{fs} B_3 (t/l)^2}{6} \quad (10)$$

where $B_3 = Pl/M_{max}$ depends on the loading configuration. The compressive strength of a foam with sandwich cell walls, σ^*_{sb}, is reached when the shear stress in the core of the sandwich equals its shear strength, τ^*_c. Setting

$$\tau^*_c = \frac{P}{B_4 lc} \quad (11)$$

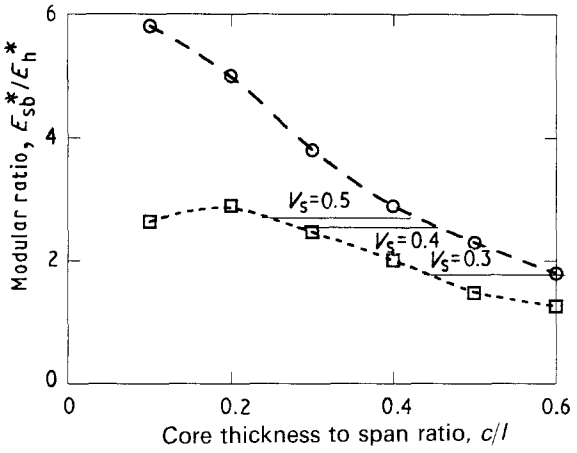

Figure 8 The ratio of Young's modulus of a cement foam with sandwich cell walls to that of a cement foam of equal density with homogeneous cell walls, E^*_{sb}/E^*_h plotted against the ratio of the core thickness to the span, c/l. (——, ---) Equation 8, (———) measured values of the modular ratio. (○) $f/l = 0.01$, (□) $f/l = 0.02$.

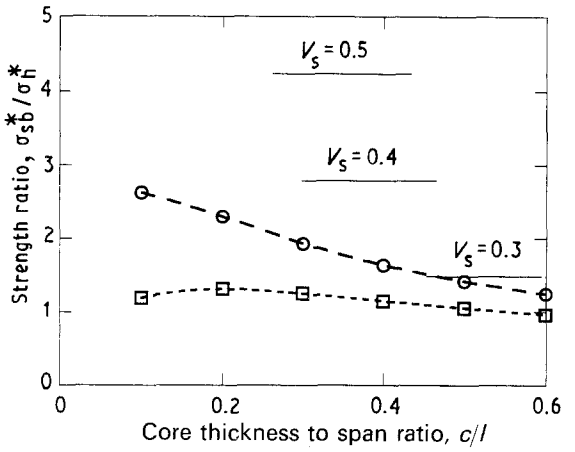

Figure 9 The ratio of the compressive strength of a cement foam with sandwich cell walls to that of a cement foam of equal density with homogeneous cell walls plotted against the core thickness to span ratio, c/l. (——, ---) Equation 13, (———) measured values of the strength ratio. (○) $f/l = 0.01$, (□) $f/l = 0.02$.

where $B_4 = P/V_{max}$, the load divided by the maximum shear force in the member, we find, referring to Fig. 7d

$$\sigma^*_{sb} = \tau^*_c B_4(c/l) \quad (12)$$

The ratio of foam strengths for sandwich and homogeneous cell walls is then

$$\frac{\sigma^*_{sb}}{\sigma^*_h} = \frac{6\tau^*_c B_4(c/l)}{\sigma_{fs} B_3 (t/l)^2} \quad (13)$$

For the loading configuration shown in Fig. 7b, $B_3 = 2$ and $B_4 = 1$. Using Equations 9 and 13 the compressive strength ratio of foams of equal mass is plotted against the core thickness to span ratio, c/l, in Fig. 9. Measured values of the strength ratio are superimposed on the figure for volume fractions of spheres of 0.3, 0.4, and 0.5; the measured strength ratios are plotted for the values of c/l assumed in Fig. 8. As expected, the strength ratio increases with increasing volume fractions of spheres, but at a faster rate than the simple model suggests. The data confirm that cement foams with a sandwich cell wall structure have improved strength over plain cement foams of the same density.

The modulus of rupture of the composite cement/polystyrene foams is plotted against density in Fig. 6a. The modulus of rupture consistently increases with increasing volume fractions of spheres. The mean modulus of rupture of a cement foam composite with 52% spheres is over two and a half times that of a plain 320 kg m^{-3} cement foam. The composite with 52% spheres has roughly equal values for the modulus of rupture and the compressive strength, suggesting that the introduction of the spheres has eliminated the presence of cracks in the microstructure. The specific modulus of rupture is plotted against volume fraction of spheres in Fig. 5b; the composite with 52% spheres has a specific modulus of rupture of almost five times that of the plain cement foam. Improvements in the modulus of rupture of the cement foams with the spheres are attributed to two factors: the presence of the EPS spheres both limits the size of cracks present in the composite and lengthens the crack path.

The introduction of 45%–50% volume fraction of 5 mm diameter expanded polystyrene spheres into a cement foam matrix produces a composite with attractive properties for use in the cores of structural sandwich panels; the properties of the composite are compared with those of other possible core materials in Table I. The density of the composite cement foam is still higher than comparable polymer foams, but this is compensated for by its much lower cost. The Young's modulus of the cement composite foams is about 140 MPa, ten times that of polymer foam cores, reducing the contribution of shear deflections in the core to the total deflection of a panel. As a result, creep is not expected to be a problem with cement/EPS composite foam core panels. The compressive and tensile strengths are roughly equal, suggesting that the largest crack within the composite cement foam is of the order of the cell size. The thermal resistance of the composite cement foam is lower than the polymers, but again, if a thicker panel is used, comparable overall R values can be achieved. Cement composite foams are more fire-resistant than polymer foams. Specimens with a surface skin of cement do not burn under a propane torch. Specimens with a cut surface, exposing the polystyrene spheres, self extinguished after the exposed polystyrene melted under the propane torch.

Additional research and development is needed to make a practical cement foam core building panel. The densities and mechanical properties achieved using the cement/polystyrene composite foam demonstrate that cement composite foams possess considerable potential for use in building panel cores.

5. Conclusions

The microstructure and mechanical properties of cement foam–polystyrene sphere composites have been measured and reported. It is possible to design the composite to produce a cellular concrete with sandwich cell walls, improving its mechanical performance. The data for the Young's modulus and compressive strength of composite cement foams suggests that the

TABLE I Comparison of core materials for building panels

Property	Polyurethane	Polystyrene	Cement foam	Cement composite foam
ρ (kg m^{-3})	32	16–32	240	192
E (MPa)	10–14	5.4–11	70	140
σ_c (MPa)	0.14–0.17	0.07–0.14	0.14	0.38
σ_t (MPa)	0.17–0.28	0.10–0.14	0.07	0.38
R (°C W^{-1})	136–180	90	45	68
Thickness for R = 680 °C W^{-1} [a] (mm)	100–125	190	375	250

[a] R = 680 °C W^{-1} is equivalent to R = 30 h ft °C/BTU per inch.

sandwich effect begins at volume fractions of spheres of 20%–30%, and that the maximum effect occurs at volume fractions of spheres of 45%–50%. Such cement foam composites have a number of properties which make them attractive for use in the cores of building panels: low cost, adequate mechanical properties, adequate thermal insulation, and good fire resistance. Additional research and development is required to make a practical cement foam core building panel.

Acknowledgements

This project has benefitted from advice and support from a number of sources, for which we are grateful. Dr Jack Germaine, Professor Leon Glicksman and Mr Steven Rudolph, MIT, and Mr Ned Glysson and Mr Leo Legatski, Elastizell Corporation of America, provided useful technical advice. The spheres used in the composite foams were provided by Neste Oy, Emerson and Cumings, and 3M at no cost. Maia Hansen, Boris Ivanovic, Warren King and Debbie Min provided assistance with specimen preparation and testing. Financial support for the project was provided by the Innovative Housing Construction Consortium at MIT: Alcan International, General Electric Plastics Division, Illinois Tool Works, Mobay Chemical Corporation, US Gypsum Corporation, and Weyerhaeuser Corporation. Fellowship support for Dr Tonyan was provided by the Program in Advanced Construction Technology at MIT, sponsored by the Army Research Office.

References

1. L. J. GIBSON and M. F. ASHBY, "*Cellular Solids: Structure and Properties*" (Pergamon Press, Oxford, 1988).
2. T. D. TONYAN and L. J. GIBSON, *J. Mat. Sci.* **27** (1992) 6371.

Received 3 January
and accepted 4 February 1992